



## OPTIMIZATION OF A HYBRID HIGH VOLTAGE ELECTRODE'S FOR 765 KV BUS- POST INSULATOR'S

G SURESH1, Dr.S.SEENIVASAN2 , P SRINIVAS RAJU, CH PRASANNA  
4.PRAVEEN KUMAR, 5.CH.HARI VARMA

EEE Department,

1Ellenki College of Engineering and Technology, Hyderabad, India

2Annamalai university Tamilnadu India

### A B S T R A C T

The designing of the high voltage electrodes such as grading rings, corona rings, and bus conductors for the station bus post insulators at extra and ultra-high voltage levels pays more attention. Improper design dimensions of high voltage electrodes engenders enhancement of electric field stresses and uneven potential distribution across the insulator which results in the catastrophic performance of station bus post insulators. The comparative research on appropriate electrode dimensions compared to existing electrode dimensions alters socio-economical benefits to the consumers as well as the design engineers. Practically it is a tedious process to obtain the optimized high voltage electrode design dimensions and their positions in the field. Therefore, a numerical method-based simulation study is adopted to estimate the electric field stress of the high voltage bus post insulator: resulting data may be subsequently used to verify and if necessary to optimize the design of grading rings and bus conductors. This paper presents the variation of the electric field stress and potential distribution at different grading ring and corona ring sizes of the 765 kV bus post insulator. The effect of variation of grading ring diameter and overall diameter at various positions in the field are investigated and compared. From the simulation data carried out, the optimized design dimension setup of the grading ring and corona ring diameters

of the 765 kV bus post insulators are suggested. Also, the simulation data tested and compared with the actual grading ring and corona ring dimensions followed by one of the manufacturing industry.

### Introduction:

Station bus post insulators are the key devices to carry the power flow in the electrical power system. The porcelain type of bus post insulators is one of the superior insulators having better electrical properties compared to polymeric type insulators [1]. Station bus post insulators may contain the 2,3,4,5 etc, units based on voltage Applications. There are two units for 400 kV bus post insulators, four units for 765 kV, and six units are used for 1200 kV bus post insulators [2]. Designing the high potential electrodes such as corona rings, grading rings, bus conductors, etc. to bus post insulators in the substation at high and extra-high voltages plays a vital role in reliable power transmission and efficiency in power systems [3]. Corona and grading rings are the major electrodes that incorporate multiple functions such as controlling the electric field stress, retaining uniform electric field and potential distribution, etc. for the any HV/EHV high voltage equipments. The position of these corona and grading rings is also very important constraint needs to cover the joints of the live end of the high voltage Device, failing which causes ardent electric field stress. The design constraints of the high voltage electrodes for EHV bus post insulators consist of

technical constraints as well as economic constraints. The design analysis of high voltage electrodes includes the estimation of electric field stress, voltage distribution across the station bus post insulator units, optimal grading ring diameter, optimal corona ring diameter overall grading ring tube diameter, overall corona ring tube diameter, and its suitable positions from the live electrode, etc. Unequal design dimensions of high voltage electrodes at high and extra-high voltages may result in uneven electric field stresses around terminals of station bus post insulators [4]. The maximum electric field stress allowed under standard atmospheric temperature, pressure is 3.00 kV/mm, beyond this value initiates electric field stress on and nearer to the live end of the electrical equipment. Failure in the estimation of this electric field stress before designing the bus post insulators for different voltage applications may affect the age of the bus post insulators [5]. This instigates the flashovers across the bus post insulators and further, it leads to complete failure of station bus post insulators [6]. Also insulators under polluted climatic conditions such as contaminated surfaces, ice loading, wet condition, etc. at higher voltage levels have a profound influence on the generation of enhanced field stress at and along with the bus post insulators [7,8]. This authenticates that, design of EHV bus post insulators with an improper selection of electrode dimensions leads to the complete shutdown of substation [9,10]. Hence, the design of corona and grading rings are essential to obtain the minimum electric field distribution, uniform potential distribution across the bus post insulator [11,12]. The designing of the grading rings involves ring diameter, overall cross-sectional diameter, and their appropriate locations. To obtain the optimized design dimensions, every design dimension needs to be tested and checked over a long period for different climatic conditions. It is a complex and tedious procedure to obtain the optimized

design dimension configuration in the field practically [15,16]. Recent advances in technology aids conducting comprehensive research using 3-dimensional simulation analysis for the given geometry configurations. Hence, this paper aims to investigate the variation of electric field and potential distribution of 765 kV bus post insulators at different electrode design dimension configurations. Therefore, this paper presents the simulation testing analysis of the proposed 765 kV bus post insulator with different corona and grading ring design configurations to attain optimized electrode design dimensions [17–19].

Several computational methods such as the boundary element technique (BET) [20], finite element technique (FET) [21], charge simulation technique (CST) [22–24], etc. are available to analyze this electric field and voltage distribution at the terminal as well as along with the units of the post insulators. In order to design the high voltage electrodes, a 3-D software named coulomb 3D [25] electrical modeling software was used to analyze the optimized design dimensions for 765 kV bus post insulators. This coulomb 3-D software [26] is allowed to design any electrical devices in a 3-dimensional view and performs the electric field calculations and voltage circulation analysis for a given desired voltage applications to the device. The boundary element method of computational technique is used in the software to evaluate the electric field stress and potential sharing along with the post insulator units. The computational results of BET offer proficient results compared to other computational methods. Because of the complex geometry cases such as high voltage insulators, bushings, C.T's, P.T's, etc. compared to the FET, CST, proposed BET serves for obtaining very accurate results. BET concentrates to estimate the electric field and potential distributions with the equipment body as its boundary points. Whereas, in the case of FET, the electric field calculations are

boundary limits are extended up to a few meters distance results in a lacuna of accuracy compared to BET. Hence, the proposed work used boundary element computational technique to obtain proficient results compared to other computational methods. This paper presents the simulation data carried out for different grading ring diameters at a suitable position along with the bus conductor and a comparison of the ring diameters. Also, the proposed work tested one of the manufacturing company grading ring design dimensions of 765 kV bus post insulators to justify the simulation data carried for obtaining the optimal dimensions. The bus conductor on the top of the stack of the insulator is considered and it offers the shielding effect of the grading ring and the designs simulated with the suitable size and length of the bus bar conductor [27].

#### Background works

Various research works are carried out elsewhere in the world to study the electric field and potential distribution of different HV/EHV bus post insulators. Among the various research works, few related works are studied to obtain enhanced performance of the proposed 765 kV bus post insulator.

C. Jing studied the comparative analysis of porcelain post insulators up to 1220 kV AC voltage levels using the boundary element method of computation available in 3-dimensional computer software. They performed the comparisons for the improvement of contamination performance, with commonly used methods of increased creepage distances, coating of hydrophobic materials, etc., and made suggestions for the performance of the type of post insulators at different high, extra, and ultra voltage levels [1]. EPRI report shows that, the design and performance analysis of different types of insulators along with post insulators above the 200 kV high voltages [2]. K.

Hou [3] presented the simulation-based algorithm-based optimization of field stress by calculating the tangential field components at critical points of the insulator. The algorithm developed by him is based on a modified charge simulation technique to compute the tangential field values on the surface of the insulator. Based on his results, he suggested optimized grading ring dimensions for composite type of insulators.

Raja Nayak presented the comparative design considerations of grading rings and corona ring to obtain the equal potential distribution and controlled field stress at terminals of the composite insulators used in UHV voltage levels. The comparative results suggest the optimized design dimensions achieve equal potential distribution and controlled field stress [4,6]. J. Koo [5] presented the maintenance of insulators under different polluted environments and at different temperature conditions. Authors R. Shi [7] and R.S. Gorur [8] also presented the performance of the ceramic and non-ceramic insulator flashover performance under different polluted and contaminated pollution conditions. They discussed the design considerations of types of insulators by applying commonly employed methods of increase in creepage distance, application of hydrophobic materials increase in leakage current flow on the surface, etc. Also, electric field calculations under ice-coated, dry, and wet conditions of insulators are considered for the flashover performance of the insulators [9].

M. Sarajlic [10] and H. Akkal [11] discussed the design considerations of high voltage electrodes like corona rings, grading rings, etc. to obtain the optimized electric field values for 1200 kV AC post insulators. They also presented the comparative analysis for different design dimensions and suggest the suitable design dimension to given applied voltage. Tiebin Zhao

pressed the electric field calculations of non-ceramic type insulators with considering the effects of transmission conductors and towers also [12]. H. El-Kishky presented the modified charge simulation method for the calculation of potential and electric field distribution for the suspension-type insulators. They performed the calculation by considering the number of smaller charge magnitudes to reduce the complexity of the calculation method [13]. Ralf Hartings presented measurements and calculations of electric fields of post insulators by the algorithm of an iterative method [14]. C. Zhang presented the modeling of insulators for given voltage applications under uneven wet conditions [15]. Also, the design modeling of insulators by considering the natural and artificial polluted conditions and study of electric field variations under these conditions are discussed [16,11]. The modeling of design considerations includes design dimensions of high voltage electrodes such as corona rings, grading rings, bus conductors, etc. [17].

C. Volat discussed the design modeling for calculations of field stress and potential sharing across the surface of the post insulator with consideration of effects of air gaps and partial arcs across the post insulators in two parts. Also, he made suggestions in design modeling under these two special effect considerations [18,19]. Many others [20– 23] presented the different computational methods such as the boundary element method, finite element technique, and charge simulation technique for calculations of an electric field as well as potential distributions for post insulator cases with suitable equations. The method of calculations suggests the application of these techniques to a given problem. The application of these methods for the calculation of electric field and voltage distributions for a given post insulator in computer software named couloJmb-3D is discussed in [25,26]. X. Yang

discussed necessary shielding effects for different design dimensions are discussed in [27]. D. Beatovic [28] and A. Carsimamovic [29] presented the necessary equations to obtain optimum electric field and potential

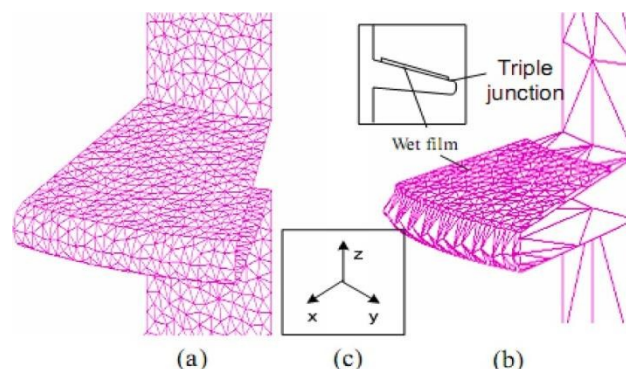


Fig. 1. Discretisation of insulator body in the boundary element method.

calculations for given electrical devices at applied voltages. The equations further help the electrical design engineers to achieve acceptable results. Also, the empirical formula for theoretical estimation of electrical field stress for analysis of electric field variations at various high and extra-high voltage levels is presented.

#### Method OF Calculation:

The method of calculation uses the boundary element method of computation for the estimation of electric field stresses and the potential allocation of the bus post insulators [28]. This method of computation

can be mostly classified under boundary methods. The boundary

$\phi(r)$  represents potential at location  $r$

$\alpha$ : is a constant and equal to 1 or 2 for two or three-dimensional problems respectively.

$\rho_s$  = Surface charge density at location  $r'$

$\Gamma$  = Border between different regions  
 $r$  = Field point and  $r'$  is source point.

$\Phi^*(r, r')$  = The fundamental solution to the potential problem.

The electrical field was calculated by estimating the potential gradient as:

$$E(K) = -\nabla \phi(r) \quad (2)$$

$$= \nabla \left[ \frac{1}{4\pi\epsilon_0} \int_0 \rho(r') \phi^*(r, r') d\Gamma(K') \right]$$

$$\epsilon_0 \int_{\Gamma}$$

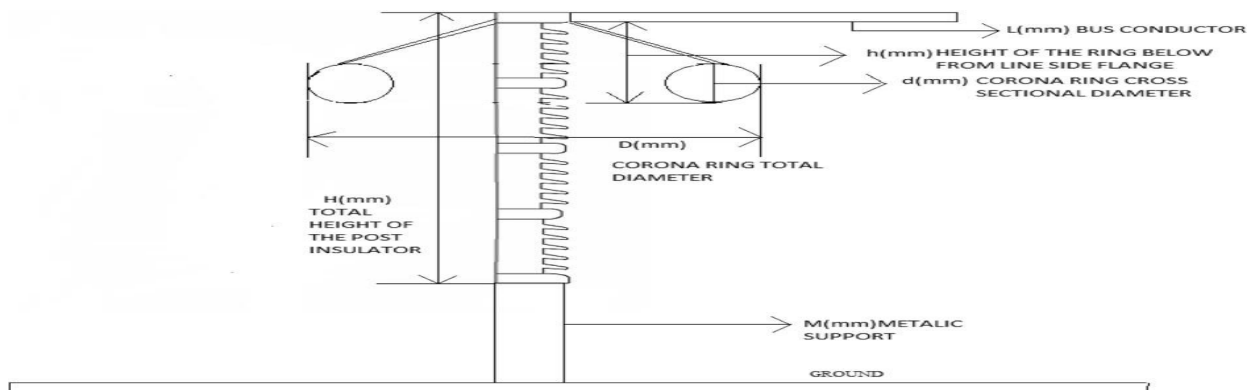
methods include charge simulation and boundary element techniques.  $= \frac{1}{4\pi\epsilon_0} \int_0 \rho(r') \phi^*(r, r') d\Gamma(r')$

To carry out the estimation of electric field stress for proposed 765

$$2\pi\sigma\epsilon_0 \int_{\Gamma} s$$

buspost insulator, boundary element method based 3-D simulation software named as COULOMB 3D was used. The

Fig. 2. The schematic diagram of the modeling of the bus post insulator (where,  $H$  = Total height of the bus post insulator in mm,  $h$  = Height of the corona ring below from the line side flange in mm,  $D$  = Corona ring total diameter in mm,  $d$  = Corona ring cross-sectional diameter in mm,  $L$  = Length of bus conductor in mm,  $M$  = Height of Metallic support above ground in mm).



various algorithm type steps are involved in software for BET method. The various steps involved in computation are: i) discretization of the body of the device,

ii) creation of device body in to regular shapes i.e square, rectangular, triangular, trapezoidal etc., iii) Assigning the potential equations iv) calculation of potential equations, v) Addition of potential equations, vi) Computation of electric field and potential magnitudes. This boundary

The accuracy of the computational simulation depends on the discretization count, shape, and allocation of boundary elements utilized.

#### Modeling OF BUS POST INSULATOR:

The modeling of bus post insulator accomplished using the 3-dimensional software named COULOMB 3D. The design model of the line post insulator for example is shown in Fig. 2. All the design dimensions of the insulator are designed in millimeters.

Voltage distribution and electric field magnitudes of the bus post insulator at D = 650 mm and D = 750 mm at h = 230 mm, h = 270 mm.

D = 650 mm, h = 260 mm							D = 750 mm, h = 260 mm					
d = 65 mm		d = 75 mm		d = 95 mm		d = 65 mm		d = 75 mm		D = 90 mm		
	Bottom corona ring	Top corona ring	Bottom corona ring	Top corona ring	Bottom corona ring	Top corona ring	Bottom corona ring	Top corona ring	Bottom corona ring	Top corona ring	Bottom corona ring	Top corona ring
Bottom point of the G ring	7.71	12.59	7.04	1.30	6.10	1.56	8.01	3.25	7.76	2.10	6.95	0.95
Top point of the G ring	1.59	7.89	0.82	7.71	0.91	6.41	2.51	7.89	2.00	7.3	1.20	6.32
Right point of the G ring	6.59	5.56	5.15	6.30	5.04	5.96	6.24	6.10	5.185	5.71	5.00	4.95
Left point of the G ring	1.99	3.98	2.442	4.51	1.82	3.82G	2.44	3.99	2.75	4.42	2.30	1.45
D = 650 mm, h = 230 mm							D = 750 mm, h = 270 mm					
d = 65 mm		d = 75 mm		d = 95 mm		d = 65 mm		D = 75 mm		d = 90 mm		
Voltage across the post (KV)		Voltage across the post (KV)		Voltage across the post (KV)		Voltage across the post (KV)		Voltage across the post (KV)		Voltage across the post (KV)		
Unit 1	219	213		214			219		215		219	
Unit 2	117	117		199			117		120		117	
Unit 3	67	70		70			67		69		67	
Unit 4	107	108		107			107		106		107	

Table 2

Voltage distribution and electric field magnitudes of the bus post insulator at D = 750 mm and D = 850 mm at h = 230 mm.

D = 750 mm, h = 230 mm							D = 850 mm, h = 230 mm					
d = 65 mm		d = 75 mm		d = 90 mm		d = 65 mm		d = 75 mm		d = 90 mm		
	Bottom corona ring	Top corona ring	Bottom corona ring	Top corona ring	Bottom corona ring	Top corona ring	Bottom corona ring	Top corona ring	Bottom corona ring	Top corona ring	Bottom corona ring	Top corona ring
Bottom point of the G ring	7.69	2.17	7.20	2.21	6.32	1.85	7.66	2.15	7.12	2.10	6.60	0.65
Top point of the G ring	1.96	8.18	2.002	7.77	1.82	6.60	1.72	8.25	2.00	7.59	0.50	6.29
Right point of the G ring	5.71	6.62	5.24	6.23	4.45	4.23	5.63	6.50	4.95	6.15	4.551	4.42
Left point of the G ring	2.66	1.00	2.48	2.70	1.92	0.96	2.65	1.64	2.02	2.52	2.10	2.03
D = 750 mm, h = 230 mm							D = 850 mm, h = 230 mm					
d = 65 mm		d = 75 mm		d = 90 mm		d = 65 mm		d = 75 mm		d = 90 mm		
Voltage across the post Units (KV)		Voltage across the post (KV)		Voltage across the post (KV)		Voltage across the post (KV)		Voltage across the post (KV)		Voltage across the post (KV)		
Unit 1	215	213		210			219		215		219	
Unit 2	118	120		118			117		120		117	
Unit 3	69	68		68			67		69		67	
Unit 4	108	109		114			107		106		107	

Table 3  
Voltage distribution and electric field magnitudes of the bus post insulator at D = 850 mm and D = 650 mm at h = 270 mm.

D = 850 mm, h = 270 mm							D = 650 mm, h = 270 mm					
d = 65 mm		d = 75 mm		d = 90 mm		d = 65 mm		d = 75 mm		d = 90 mm		
	Bottom corona ring	Top corona ring	Bottom corona ring	Top corona ring	Bottom corona ring	Top corona ring	Bottom corona ring	Top corona ring	Bottom corona ring	Top corona ring	Bottom corona ring	Top corona ring
Bottom point of the G. ring	7.04	1.30	7.71	1.92	6.10	1.56	7.04	1.30	7.80	1.92	6.10	1.56
Top point of the G. ring	0.82	7.80	1.841	7.32	0.91	6.41	0.82	7.71	1.84	7.32	0.91	6.41
Right point of the G. ring	5.15	6.30	5.70	5.61	6.38	6.21	5.15	6.30	5.70	5.61	4.56	5.01
Left point of the G. ring	2.42	4.51	2.61	2.13	1.82	3.82	2.42	4.51	2.612	2.13	1.82	3.82
D = 850 mm, h = 270 mm							D = 650 mm, h = 270 mm					
d = 65 mm		d = 75 mm		d = 90 mm		d = 65 mm		d = 75 mm		d = 90 mm		
Unit	Voltage across the post (KV)	Unit	Voltage across the post (KV)	Unit	Voltage across the post (KV)	Unit	Voltage across the post (KV)	Unit	Voltage across the post (KV)	Unit	Voltage across the post (KV)	
Unit 1	219	Unit 2	213	Unit 3	214	Unit 1	215	Unit 2	213	Unit 3	210	
Unit 2	117	Unit 3	117	Unit 4	199	Unit 1	118	Unit 2	120	Unit 3	118	
Unit 3	67	Unit 4	70		70	Unit 4	69		68		68	
Unit 4	107		108		107		108		109		114	

Table 4  
Comparison of optimized and manufacturing industry electrode design dimensions.

Item/Description	Corona ring cross-sectional diameter d (mm)	Corona ring cross-sectional diameter D (mm)	Height of the corona ring below from the line side flange h (mm)
Manufacturing Industry electrode design dimensions	95	650	260
Optimized electrode design dimensions	75	750	230

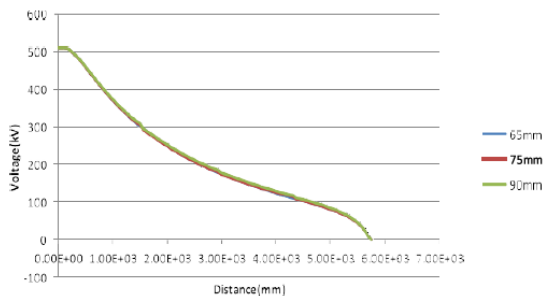


Fig. 3. Voltage distribution of 765 kV post insulator at D = 750 mm and h = 230 mm.

Onset gradient is calculated using the empirical formula [29]

$$E = 32.4 * m * R_{eq}^{-0.3} \text{ kV/cm} \tag{3}$$

where

$$E = \text{Electric field in kV/cm}$$

$$R_{eq} = 2 * R_1 * R_2 / (R_1 + R_2) \text{ in mm}$$

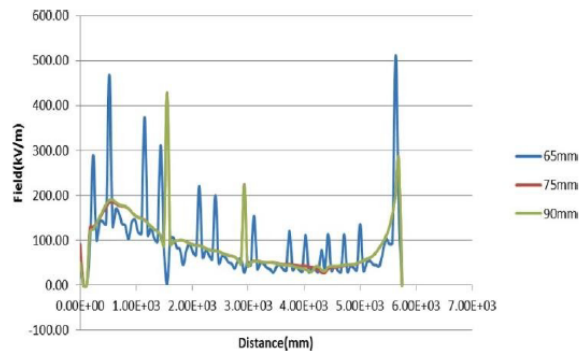


Fig. 4. Electric field distribution 765 kV post insulator at D = 750 mm and h = 230 mm.

$R_1$  = radius of the corona ring in mm  
 $R_2$  = cross sectional radius of the ring in mm  
 $m$  = roughness factor (for all cases it is considered as 0.9)

To optimize the high voltage electrode dimensions, different case studies have been carried out by varying various parameters viz., D, d, h which are shown in the following case studies. For 400 kV Bus post insulator, the number of porcelain post insulator units used is four. In all cases, H is held constant at 5.750 m, M at 2.5 m, and L at 2.5 m. Also in all cases, two rings are considered at the top and bottom side of the terminal flange of the 765 kV post insulator.

**Results**

*Case 1*

The simulation study of estimation of the variation of electric field and potential distribution has been carried out for different electrode configurations including the Gdesign dimensions of D = 650 mm, h =

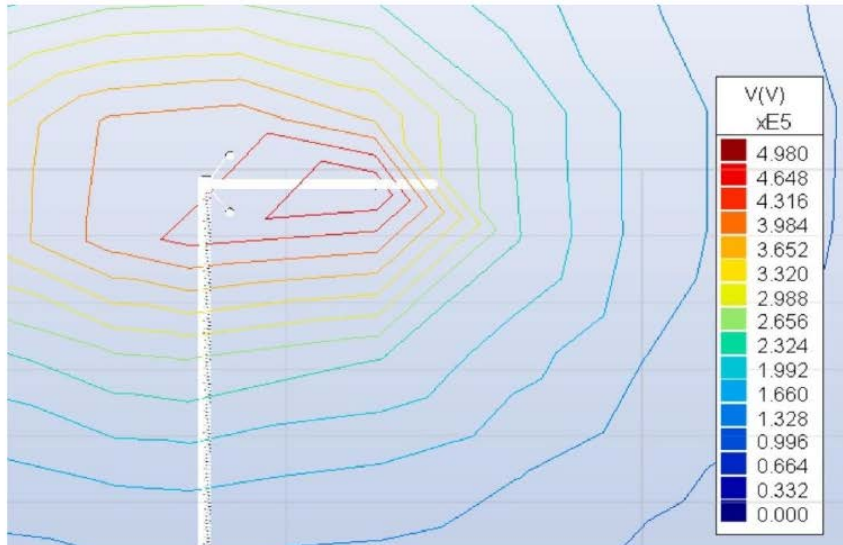


Fig. 5. Voltage contours of 765 kV post insulator at D = 750 mm and h = 230 mm.

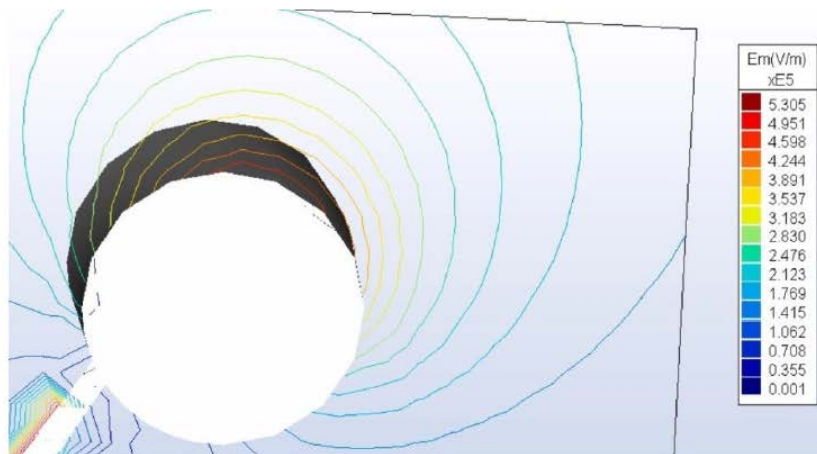


Fig. 6. Electric field contours of 765 kV post insulator at d = 75 mm, D = 750 mm, h = 230 mm.

mm ar d =92 mm, provided by the manufacturing industry. The high voltage is applied to the top electrode of the post insulator and it is 510 kV i.e.  $(765/\sqrt{3}) * 1.11$  and 0 voltage is applied to the bottom electrode. The below table lists the comparison of field stress values for different corona ring diameters, grading ring diameter, voltage distribution of each post (number of poSsts=4) w. r. t ground and a cross-sectional diameter of D dimensions. The present simulation study is aimed to observe the electric field and potential distribution for reduced to ring diameter of d =90 mm compared to

manufacturing company designed dimension of d =95 mm to obtain optimized design configuration comparison.

In this case, the maximum electric field magnitude calculated for given design dimensions of D= 650 mm, and D=750 mm using the empirical formulae (3) for both above design setups are 9.25 kV/cm

9.17 kV/cm respectively. It is also observed from Table 1, the ring diameter d =75 mm shows better electric field



magnitudes of 7.81 kV/cm and 7.76 kV/cm respectively compared to the other two ring diameters  $d = 62$  mm,  $d = 90$  mm. Also, the applied high voltage is distributed across the four-post insulator units with respect to the applied voltage to its distance allocation from the live voltage end for both design setups of  $D = 740$  mm,  $D = 650$  mm respectively. But, it is noticed from Table 1 that, higher potential distribution across the fourth insulator unit compared to the third unit, this may be attributed that due to the ground stray capacitance effect.

### Case 2

In addition to the above case study 1, The electric field magnitudes are calculated and tested for the design dimension setups of  $D = 750$  mm,  $h = 230$  mm and  $D = 850$  mm,  $h = 270$  mm. The below table lists the comparison of field stress values for different corona ring diameters, grading ring diameter, voltage distribution of each post (number of posts = 4) w. r. t ground.

The maximum electric field stress is calculated using the empirical formulae (3) for design set up of  $D = 750$  mm,  $h = 102.5$  mm is 8.21 kV/cm. It is also observed from Table 2, at  $D = 750$  mm and  $h = 230$  mm, the ring diameter  $d = 75$  mm shows a better electric field magnitude of 7.77 kV/cm compared to the other two rings diameters  $d = 65$  mm,  $d = 95$  mm. Similarly, for the design case study of  $D = 850$  mm, the maximum electric field stress calculated using empirical formulae (3) is 9.25 kV/cm and it is observed from Table 2 the ring diameter  $d = 75$  mm shows a better electric field magnitude of 7.59 kV/cm compared to the other two ring diameters  $d = 65$  mm,  $d = 90$  mm. Furthermore, like case study 1, a similar potential allocation is observed across the four-post insulator units with minor potential magnitude.

### Case 3

In this case,  $D$  and  $h$  varied compared to the above two case studies. The below table lists the comparison of field stress values for different corona ring diameter, grading ring diameter, voltage distribution of each post (number of posts = 4) w. r. t ground.

Furthermore, the electric field magnitudes are calculated and tested for the design dimension setups of  $D = 650$  mm,  $h = 270$  mm and  $D = 850$  mm,  $h = 270$  mm. The maximum electric field magnitude calculated using the empirical formulae (3) for both above design setups are 9.25 kV/cm 9.25 kV/cm respectively. It is noticed from Table 3, the ring diameter  $d = 75$  mm confirms better electric field magnitudes of 7.71 kV/cm and 7.32 kV/cm respectively compared to the other two ring diameters  $d = 65$  mm,  $d = 90$  mm. Additionally, like above case studies 1 and 2, a similar potential allocation is observed across the four-post insulator units with minor potential magnitude. Also, the comparison table of variation of electric field and potential distribution for obtained optimized electrode dimensions and electrode dimensions given by manufacturing industry is shown in below table 4.

From the above three case studies presented, it is evident that a linear

potential distribution and nonlinear electric field distribution across the four posts of the insulator. The electric field magnitudes are shown critical for grading ring diameter of 60 mm compared to 75 mm and minimum for 90 mm compared to 75 mm. This attributes that, the ring diameter  $d = 75$  mm showing satisfactory results of the electric field magnitude values compared to the other two ring diameters  $d = 65$  mm and  $d = 90$  mm respectively for a given 765 kV bus post insulator. Therefore, from the above simulation data carried out, the optimum grading ring dimensions are obtained at a ring diameter of  $d = 75$

mm and a cross-sectional diameter of  $D = 750$  mm at a vertical distance of  $h$

$= 230$  mm. The variation and contours of voltage distribution and

electric field distribution for 765 kV bus post insulator at optimized grading ring dimensions with the axis of symmetry. Also, from the simulation data presented in above case studies, it is proved that simulation based study support of practical testing of high voltage equipments shows significant support to the design engineers.

### Conclusion

The optimum design of high voltage electrodes of 765 kV porcelain bus post insulator using 3-D computational based simulation studies are carried out and the following directions inferences are drawn from the data presented:

- The design dimensions of the grading ring given by the manufacturer at the high voltage end considered for the study resulted in an electric field within the limit magnitude of 3.0 kV/mm at both metal end fittings
- The potential distribution across the 765 kV bus post insulator units is linear in all grading ring diameter dimensions.
- The electric field magnitude of 65 mm grading ring diameter shows maximum and minimum at 90 mm ring diameter compared to the 75 mm grading ring diameter. Hence ring diameter  $d = 75$  mm is contemplated as a techno-economic design dimension.
- The minimum electric field stress magnitude of 0.5 kV/mm for ring design configuration of  $d = 75$  mm,  $D = 750$  mm at  $h = 230$  mm compared to ring design configuration considered by the manufacturing company at  $d = 95$  mm,  $D = 650$  mm at  $h = 260$  mm. This confirms

that the ring diameter  $d = 75$  mm with overall ring diameter  $D = 750$  mm suggests the optimal design dimensions to meet socio-economical factors.

- Therefore, for 765 kV bus post insulators, the optimal design dimensions are arrived at the ring diameter of  $d = 75$  mm, the overall cross-sectional diameter of  $D = 750$  mm, and the vertical distance of the grading ring at  $h = 230$  mm.

### Declaration of Competing Interest

The authors declare that they have no known competing financial interests or personal relationships that could have appeared to influence the work reported in this paper.

### Acknowledgment

The authors would like to thank the High Voltage Division, CPRI Hyderabad for conducting experimentation and management of Lakir-eddy Bali Reddy College of Engineering for permitting to publish this paper.

### References

- [1] C. Jing, Q. Shanshan, L. Jinxiang, W. Xiong and P. Zongren, "Research of Grading Ring for High Altitude 500 kV Compact Transmission Line," 2018 IEEE International Conference on High Voltage Engineering and Application (ICHVE), Athens, Greece, 2018, pp. 1-4, DOI: 10.1109/ICHVE.2018.8641899.
- [2] Comber MG, Doyle JR, Schneider HM, Zaffanella LE. Three-phase testing facilities at EPRI's project UHV. IEEE Trans Power Apparatus Systems 1976;95(5):1590-9. <https://doi.org/10.1109/T-PAS.1976.32258>.
- [3] K. Hou, W. Li, L. Ma, Y. Cheng and L. Jin, "Multi-objective structural optimization of UHV composite insulators based on

pareto dominance,” 2018 12th International Conference on the Properties and Applications of Dielectric Materials (ICPADM), Xi'an, China, 2018, pp. 657-661, doi: 10.1109/ICPADM.2018.8401103.

[4] M. Raja Nayak, P.V.SAditya, S.Kirankumar, M. NarayanaNayak “Optimization of Grading Rings for Suspension Type Composite Insulators used in UHVDC Transmission System”, Journal of Advanced Research and Dynamic Control Systems, vol 10 special issue, pp: 2575-2580, November 2018.

[5] J. Koo, W. Shin, D. Oh, R. Hwang and B. Lee, “Comparison of Surface Flashover Characteristics of Rod and Rib Type Post Insulator for EXtra-High Voltage Superconducting Fault Current Limiter,” in IEEE Transactions on Applied Superconductivity, vol. 27, no. 4, pp. 1-5, June 2017, Art no. 7700805. DOI: 10.1109/TASC.2017.2667892.

[6] Jialong Wang, Z. Peng, Hao Wu, Hongwei Deng, Hao Liu and Chuang Wang, “Electric field calculation and grading ring design for 330kV terminal tower with composite cross-arms,” 2016 IEEE International Conference on Dielectrics (ICD), Montpellier, France, 2016, pp. 346-349, doi: 10.1109/ICD.2016.7547615.

[7] R. Shi, J. Wang, B. Yue, Z. Liu, Z. Wu and Z. Peng, “Electrical field calculation and optimization of suspension insulator with cone conformation in valve hall,” 2018 12th International Conference on the Properties and Applications of Dielectric Materials (ICPADM), Xi'an, China, 2018, pp. 602-605, doi: 10.1109/ICPADM.2018.8401090.

[8] He L, Gorur RS. Source strength impact analysis on insulator flashover under contaminated conditions. IEEE Trans Dielectr Electr Insul 2016;23(2):1005–11.

<https://doi.org/10.1109/TDEI.2015.005264>.

[9] Olsen RG, Zhao T, Comber MG. Discussion of “Calculation of electric field and potential distribution along nonceramic insulators considering the effects of conductors and transmission towers” [Closure to discussion]. IEEE Trans Power Delivery 2000;15(4):1353–4. <https://doi.org/10.1109/61.891582>.

[10] Sarajlic M, Kitak P, Pihler P. New design of a medium voltage indoor post insulator. IEEE Trans Dielectr Electr Insul 2017;24(2):1162–8. <https://doi.org/10.1109/TDEI.2017.005947>.